TWO DIMENSIONAL THEORY OF FLUCTUATION REFLECTOMETRY DIAGNOSTICS

Gusakov E.Z., Yakovlev B.O.

Ioffe Institute
Polytechnicheskaya 26, 194021 St.Petersburg, Russia

Fluctuation reflectometry is a widely used technique providing information on the plasma turbulence [1]. Technical simplicity and operation at a single access to plasma are among its merits, which however cause interpretation problems related to localization of measurements and wave number resolution. The performance of O-mode fluctuation reflectometry is investigated in the present paper in the framework of 2D linear theory. The scattering signals are analyzed in detail for regular island-like density perturbation and for statistically homogeneous density turbulence. In the first case the explicit expression is derived for arbitrary angle of the probing wave incidence, where as in the second case the cross correlation function in the radial correlative reflectometry is calculated numerically for different turbulent spectra.

Following the approach of [2] fluctuation reflectometry signal is represented as a superposition of signals, produced by density spectral harmonics $\delta n_{q,\kappa}$

$$A_S(\omega)=\frac{2e^2\ell^2}{mc^2}\sqrt{P_i}\int\frac{dk_y d\kappa dq}{(2\pi)^3}f(k_y)f(q-k_y)C(\kappa,q,k_y)e^{i\Psi}\delta n_{q,\kappa} \quad (1)$$

where κ and q are radial and poloidal fluctuation wavenumbers;

$$f(k_y)=2\sqrt{\pi\rho}\exp\left[-(k_y-k_p)^2\rho^2/2\right] \quad (2)$$

is the antenna diagram, supposed to be Gaussian; the phase of scattered wave for the probing in direction of density gradient $\left((\omega\rho/c)^2\gg 1, k_p \ll \omega/c\right)$ takes the form

$$\Psi\simeq\frac{4}{3}\frac{L\omega}{c}-\frac{Lc}{\omega}\left[k_y^2+(q-k_y)^2\right]+\frac{1}{2}\left(\frac{c}{\omega}\right)^3 L\left[k_y^4+(q-k_y)^4\right]; \quad (3)$$

$C(\kappa,q,k_y)$ is the scattering efficiency obtained for linear density profile $n_e(x)=n_c x/L$ in [2]. It is given for $\kappa L\gg 1$ by asymptotic expression

$$C=-2\pi\sqrt{i\pi/\beta}\exp\left\{i\left[\beta^3/12-\beta\sigma-\delta/4\beta\right]\right\}, \quad (4)$$

where $\beta=\kappa\ell$, $\delta=\ell^4 q^2(q-2k_y)^2$, $\sigma=-\ell^2\left[k_y^2+(q-k_y)^2\right]$, $\ell=\left(Lc^2/\omega^2\right)^{1/3}$. In the case $\kappa L\leq 1$ the growth of C with decreasing κ saturates at the level $C=-4\pi i\sqrt{L/l}$.

The island-like density perturbation. Standard probing.

In the case of island-like density perturbation localized along the radial coordinate x

$$\delta n(x,y)=n_f\exp\{-\frac{(x-x_f)^2}{w^2}\}\cos\left[q_f(y-y_f)+\kappa_f(x-x_f)\right] \quad (5)$$

the integration in (1) is easily carried out using the saddle point method. For a wide island ($w>l$, $\kappa_f l<1$) situated far enough from the cut off ($L_q-x_f>w$, $L_q=L\left[1-(qc/2\omega)^2\right]$) in large plasma ($L>\rho^2\omega/2c$) the corresponding expression takes the following form

$$A_s=\left(\frac{\omega}{c}\right)^{3/2}\frac{\pi w\rho\sqrt{P_i}}{2\sqrt{L_q-x_f}}\sum_{m=-1}^{m=1}me^{F_0}\left[e^{F_1}-i\sqrt{2}e^{F_2}\right], \text{ where} \quad (6)$$

$$F_0 = -\rho^2\left(\frac{mq_f}{2}-k_p\right)^2 + i\frac{4L\omega}{3c} + im\left(q_f y_f + \pi\right) + iL\frac{q_f^2 c}{2\omega}\left[1+\frac{1}{2}\left(\frac{q_f c}{2\omega}\right)^2\right] + i\frac{\pi}{4} \qquad (7)$$

$$F_1 = -\frac{\left(L_q - x_f\right)^2}{w^2} + im\kappa_f\left(x_f - L_q\right) \qquad (8)$$

$$F_2 = -\frac{w^2}{4}\left(m\kappa_f + \frac{q_f^2 c}{2\omega}\right)^2 - \frac{\left(q_f\rho\right)^2}{4}\left[\frac{L_q - x_f}{L} + i\frac{w^2}{2L}\left(m\kappa_f + \frac{q_f^2 c}{2\omega}\right)\right] + i\frac{q_f^2 c}{2\omega}\left(L_q - x_f\right) \qquad (9)$$

The scattering signal, given by (7) is composed from localized response of the cut off represented by term proportional to $\exp(F_1)$ and non-localized volume scattering, produced by spectral component of perturbation possessing long radial scale

$$\kappa = -q_f^2 c/2\omega . \qquad (10)$$

This volume input is given by terms proportional to $\exp(F_2)$. It is suppressed in the case $\exp\left[-\frac{w^2}{4}\left(m\kappa_f + \frac{q_f^2 c}{2\omega}\right)^2\right] << 1$, when spectral components satisfying (10) are poorly represented in the spectrum of the island. The dependence (7) of the scattering signal on the island poloidal wave number and radial position is shown in Fig.1 a,b for traditional fluctuation reflectometry. As it is seen, the signal is only observable for fluctuations within the antenna diagram ($q \le 2/\rho$). It is maximal for the island in the cut off vicinity ($x_f \approx L_q$), but decrease slowly for ($x_f < L_q$) due to small angle scattering in the volume, that cause the spatial resolution problems.

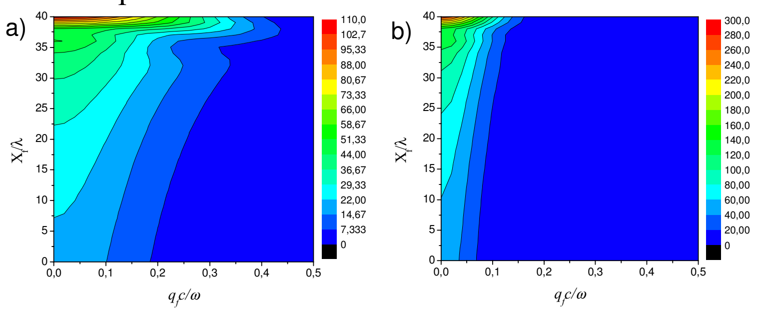

Fig. 1 . $|A_s|$ *versus* x_f/λ *and* $q_f c/\omega$ *for* $k_p = 0$, $L = 40\lambda$; $\kappa = 0.08\,\omega/c$, $w = 4\lambda$, $\lambda = 2\pi c/\omega$, $\rho_a = 1.25\lambda$, $\rho_b = 3.25\lambda$

Radial correlative reflectometry.

The volume scattering produced by long radial scales leads to wave number resolution problems as well [3]. According to analyzes of [3], based upon the asymptotic expression (4), the cross-correlation function of scattering signals at two probing frequencies decreases very slowly as $\left\langle A_S(\omega_0) A_S^*(\omega)\right\rangle \sim \ln[4\omega/\Delta\omega]$ with the frequency mismatch $\Delta\omega = \omega - \omega_0$. This conclusion is confirmed in the present paper using the general expression for the scattering efficiency [2], accounting for the growth saturation at $\kappa L \le 1$. The cross correlation function is expressed in terms of fluctuation wave number spectrum $|\delta n|^2_{q,\kappa}$ as

$$\left\langle A_S(\omega_0) A_S^*(\omega)\right\rangle = \frac{2P_i\rho^2 L}{\pi}\left(\frac{\omega}{c}\right)^3 \iint d\kappa dq \exp\left\{-\frac{(q\rho)^2}{2} + i\frac{2\Delta\omega}{\omega}\left[\frac{q^2 c}{4\omega} + \kappa - \frac{2\omega}{c}\right]L\right\}\frac{|\delta n|^2_{q,\kappa}}{n_c^2}|I(\alpha)|^2 , \qquad (11)$$

where $I(\alpha) = \int_0^1 \exp\left(i\alpha\eta^2\right)d\eta$; $\alpha = L\left(\kappa + q^2 c/2\omega\right) + i(q\rho)^2/4$. The dependence of coherence $K(\omega_0,\omega) = \left|\left\langle A_s(\omega_0) A_s^*(\omega)\right\rangle\right| / \left\langle |A_s(\omega_0)|^2\right\rangle$, on the normalised frequency shift $\Delta\omega QL/2\pi\omega$ is shown in Fig.2 a,b for the gaussian wave number spectrum (*γ=0*)

$$|\delta n|^2_{q,\kappa} = \frac{4\pi(\delta n)^2}{Q^2}\exp\left[-\left(\kappa^2+q^2\right)/Q^2\right]\left[\frac{\kappa^2}{\kappa^2+(\pi/4L)^2}\right]^{\gamma/2}, \qquad (12)$$

possessing different width Qc/ω. As one can see in Fig.2a the decay of the coherence is very slow in large plasmas, at $L/\lambda = 100$. The coherence is higher than 0.8 at frequency shift $(\Delta\omega/\omega) \simeq (QL)^{-1}$, corresponding to cut offs separation equal to the turbulence coherence length. Such a high level of coherence was found for all Q values under investigation, thus making wave number resolved measurements impossible.

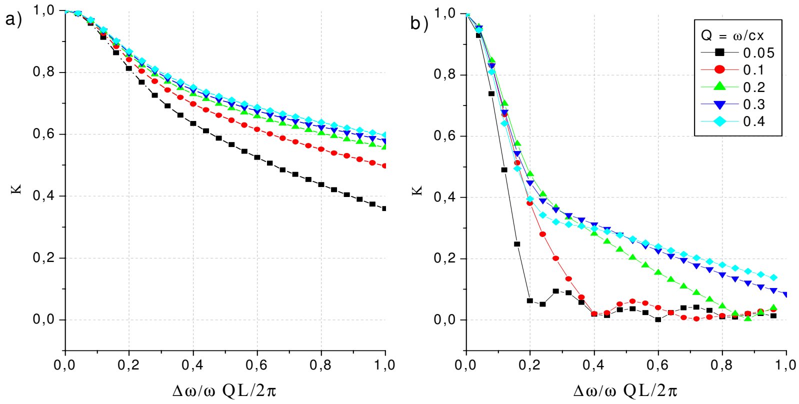

Fig. 2 *Coherence versus normalized frequency shift* a) $L/\lambda = 100$, b) $L/\lambda = 10$

In the modest size plasmas, at $L/\lambda = 10$, the calculation predictions are more favourable for the correlation technique. The volume scattering efficiency growth saturates at $\kappa = Q^2c/2\omega < L^{-1}$, making the cut off response dominant for $Q^2Lc/2\omega < 1$. As it is seen in Fig.2b the coherence decay is quick for $Qc/\omega =$ 0.05; 0.1, satisfying the above condition, but it is still slow for $Qc/\omega \geq$ 0.2, where the opposite condition is fulfilled.

In the case γ=1 in (12), the long radial scales $\kappa \leq L^{-1}$ are suppressed in the turbulence spectrum and the prospects for wave number resolution further improves. As it is seen in Fig.3a, the coherence decay quickly for $Qc/\omega =$ 0.05; 0.1 already in large plasmas, moreover the decay is fast for all scales in the modest size case (see Fig.3b). The second maximum in the dependences in Fig.3b accounts for two scales existing in the turbulence spectrum for *γ=1.*

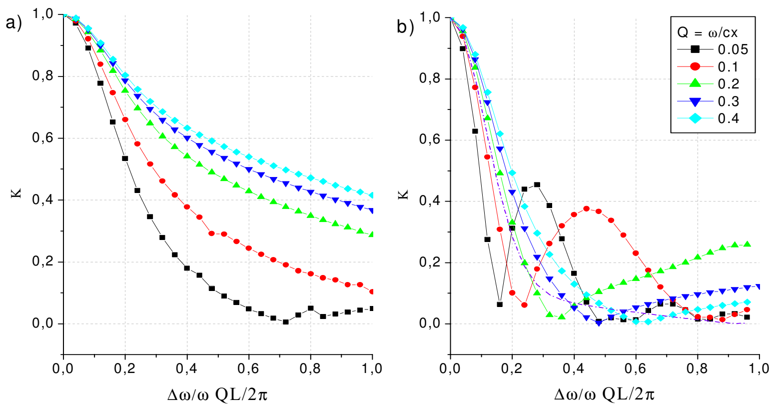

Fig. 3 *Coherence versus normalized frequency shift* a) $L/\lambda = 100$, b) $L/\lambda = 10$

The island-like density perturbation. Oblique probing.

Additional possibilities for spatial and wave number resolution improvement are predicted by expression (6) in the case of oblique probing ($k_p \neq 0$). This technique, utilizing microwave backscattering was proposed recently as Doppler reflectometry for investigation of plasma poloidal rotation [4,5]. According to (6) in this case the maximal scattering amplitude is achieved for $k_p = \pm q_f/2$. The poloidal wave number resolution, given by $\delta q \approx \rho^{-1}$, improves with growing probing beam width. Simultaneously the volume scattering far from the cut off is suppressed by antenna diagram effect described by $\exp\left[\left\{-(q_f\rho/2)^2\left[(L_q - x_f)/L\right]\right\}\right]$. This effect was first mentioned and explained in [2], where the standard fluctuation reflectometry was treated. Unfortunately in the standard case the large width of the antenna beam $q_f\rho \gg 1$ can not improve the spatial resolution because the response of cut off is simultaneously suppressed as $\exp\left[-(q_f\rho)^2/4\right]$. On contrary, in the case of oblique probing at $k_p = \pm q_f/2$ the cut off response is unaffected, where as the volume response is suppressed for $L_q - x_f > 4L/(q_f\rho)^2$. The diagnostic performance improvement with growing ρ is demonstrated in Fig.4a,b in the most unfavourable case, when the volume scattering effect is not suppressed due to the Bragg resonance mismatch at $k_p = \pm q_f/2$. The evident improvement of spatial resolution at $\rho_b = 3.25\lambda$ is seen in Fig.4b compared to Fig.4a and Fig.1 a, b.

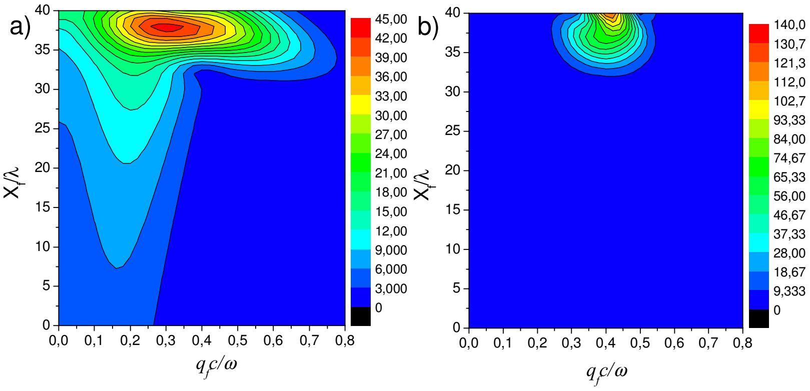

Fig. 4 $|A_s|$ *versus* X_f/λ *and* $q_f c/\omega$ *for* $k_p = 0.2$, $L = 40\lambda$; $\kappa = 0.04\,\omega/c$, $w = 4\lambda$, $\rho_a = 1.25\lambda$, $\rho_b = 3.25\lambda$

Conclusions.

According to 2D linear theory the volume small angle scattering from long radial scale component of density turbulence complicates interpretation of standard fluctuation reflectometry data, leading to degradation of spatial and wave number resolution. The spatial resolution improves drastically for so called Doppler reflectometry, utilizing oblique probing with wide microwave beam. It is likely that performance of radial correlation reflectometry will improve as well for oblique incidence.

Acknowledgements.

This work was supported by grants of RFBR 01-02-17926, 00-15-96762, RFBR-NWO, INTAS 97-11018, and by Contract of Ministry of Science of Russia.

References.

1. R.Nazikian, E.Mazzucato. Rev. Sci. Instrum. (1995), 66, 392.
2. E.Z.Gusakov, M.A.Tyntarev. Fusion Engineering and Design (1997), 34-35, p.501.
3. E.Z. Gusakov et.al. Proc.EPS Conf on Contr. Fusion and Plasma Phys. p.428, (2000)
4. Bulanin V.V. et.al. Plasma Physics Reports, v. 26, p 813, (2000).
5. XL Zou et.al. Proc. EPS Conf on Contr. Fusion and Plasma Physics, p.1041, (1999).